



Physical Properties of Shaly - Sand Reservoirs: Saffron Field, Offshore Nile Delta, Egypt

Nahla A. El Sayed¹⁾, Abdel Moktader A. El Sayed^{2*)}, Osama Moselhy³⁾

¹⁾ Egyptian Petroleum Research Institute, Exploration Department, Nasr City, Egypt

^{2*)} Ain Shams University, Faculty of Science, Department of Geophysics, Cairo, Egypt; email: moktader76@yahoo.com

³⁾ Khalda Oil Company., Department of Petrophysics, Cairo, Egypt

<http://doi.org/10.29227/IM-2024-01-10>

Submission date: 11.4.2023 | Review date: 27.4.2023

Abstract

The Saffron gas Field is in the Scarab-Saffron Development Lease in the offshore Nile Delta. It was discovered by the Saffron-1 exploration well drilled in 1998 and appraised by Saffron-2 and Sapphire-3 wells. Saffron is a stacked channel system and consists of 6 different reservoirs with differing levels of connectivity between them. It can be interpreted as deep-water canyon fill deposits on a delta-front slope. Some physical properties of 4 full diameter core samples (approximately 164 core plugs) obtained from the Saffron-2 borehole were petrophysically analysed. Helium porosity, horizontal and vertical permeability, grain density and electrical resistivity were laboratory measured. Several bivariate plots were accomplished such as porosity- permeability; grain density, formation resistivity factor; cementation exponent and Winsaur's multiplier (α) as well. Several regression line equations with robust coefficient of correlations were obtained to be used for reservoir characterization. On the other hand, numerous frequency histograms were built for most of the measured reservoir parameters to determine their type of distribution and other statistical parameters. Some important relations like cementation exponent versus multiplier (α) are performed which improves Archie's general equation and subsequently the reservoir fluid saturation (S_w and/or S_h). The lack of stratification in sedimentary section represented by core numbers 4&5 of Saffron-2 well have severe consequences on measured reservoir parameters especially exposed by the porosity-permeability relation.

Keywords: physical properties, shaly-sand reservoir, saffron field, porosity, permeability, egypt

Introduction

The Saffron Field is located on the North-Western margin of the Nile Delta, approximately 100km offshore (Fig. 1). Saffron field is one of the major Pliocene gas fields in the offshore Nile Delta, Egypt in WDDM concession with approximately 2 TCF GIIP. The field is in the Scarab-Saffron Development Lease and was discovered by the Saffron-1 exploration well in 1998 and appraised by Saffron-2 and Sapphire-3 wells. Saffron is a stacked channel system and consists of 6 different reservoirs with differing levels [1, 2, 3] of connectivity between them. Nominally, Channels A North, B, C and E (including the sheet sand) are termed Saffron North Complex, then there are the separate A South Channel and Channel 11.

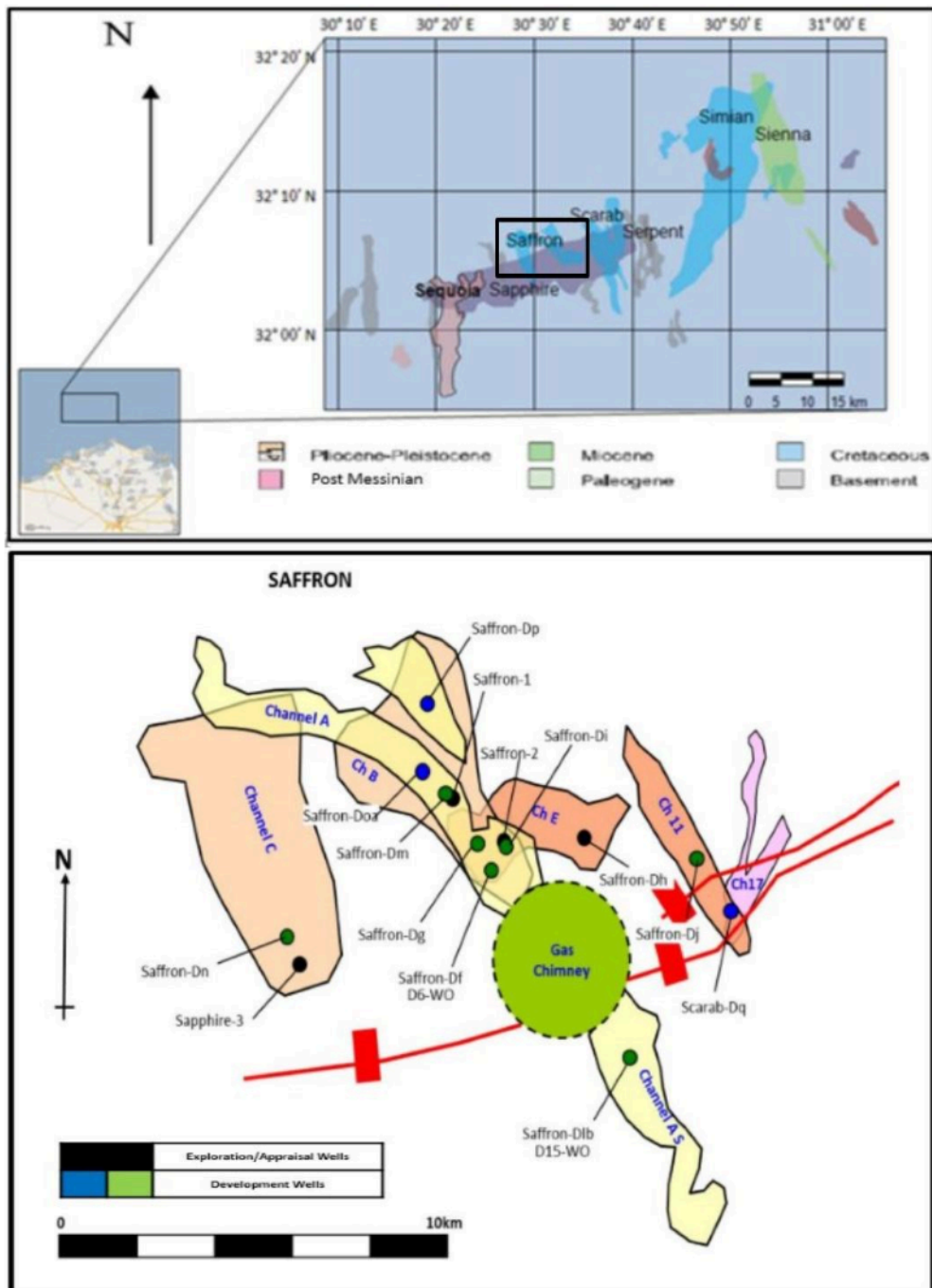


Fig. 1. Location map of the Saffron field

The Saffron reservoirs were encountered in the Pliocene sandstones of the El Wastani Formation [4, 5, 6] which can be interpreted in terms of a Pliocene deep-water canyon fill deposited on a delta-front slope. It lies along strike from several analogous canyon systems which constitute the reservoirs of the WDDM succession. The general stratigraphy of Saffron field is shown in (Fig. 2), which is related to El the Wastani Formation of late Pliocene age [7, 8, 9]. The Saffron reservoir is a heterogeneous succession of sandstones and mudstones organised into a broad upward-fining succession. High quality, blocky sands occur at the base, while the upper part of the section is characterised by apparently isolated sand bodies encased in thin-bedded sands and mudstones [10, 11]. **The aim of this paper is to investigate the** petrophysical properties of the reservoir rocks through measuring of petrophysical important parameters such as porosity, shale volume, permeability, water saturation and hydrocarbon saturation in each of studied wells.

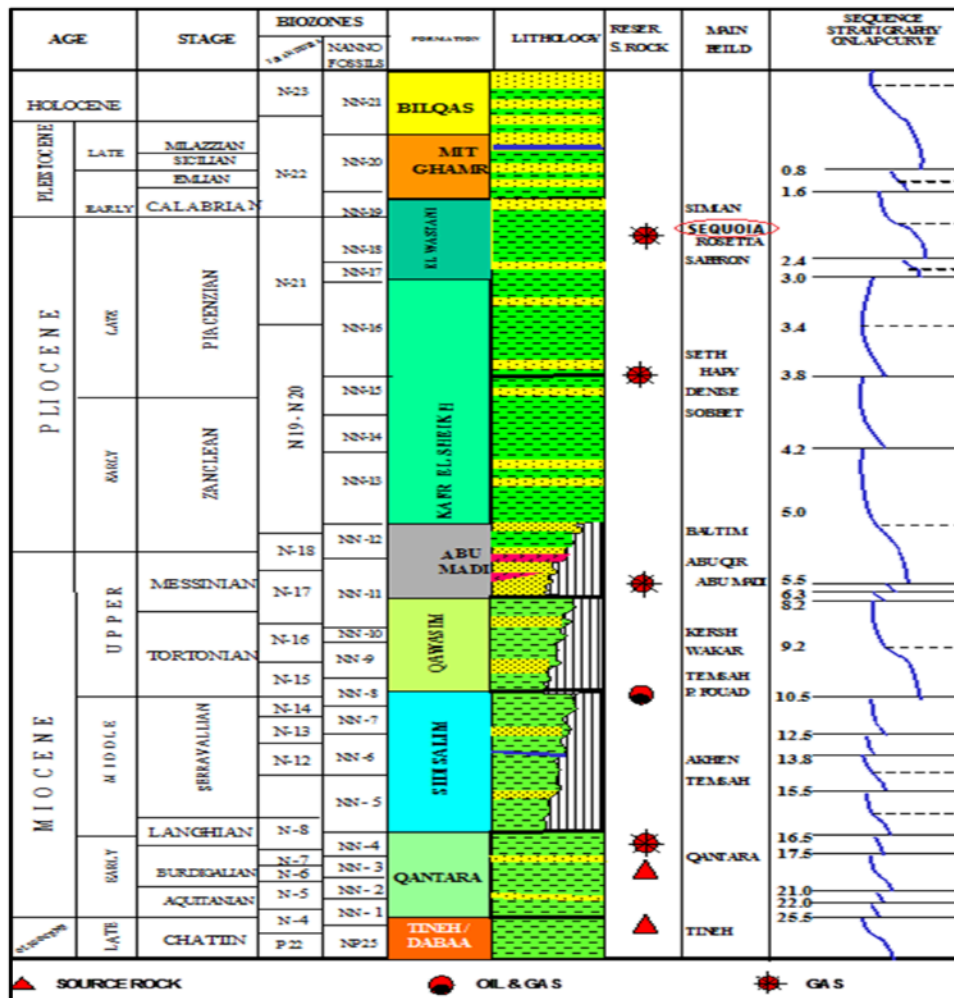


Fig. 2. The general stratigraphy of Saffron field

Methodology

The laboratory measurements of the Saffron-2 field core samples (C2,3,4&5) were started with sample preparation and then core porosity, permeability, density, and γ -ray intensity of the obtained cores. The laboratory methods are explained as:

Porosity, Density and Permeability Measurements

Porosity is measured using Helium porosimeter with matrix cup core holder for grain volume (V_g) estimation [12] Porosity (\emptyset) is calculated by the following equation:

$$\emptyset = (1.0 - V_g) / V_b \quad (1)$$

Where: \emptyset , is the porosity fraction, V_g , is the grain volume cm^3 and V_b , is the bulk volume of the sample in cm^3 .

The grain and bulk density are measured through porosity laboratory determination as:

$$\rho_g = W_d / V_g \quad (2)$$

$$\text{And } \rho_b = W_d / V_b \quad (3)$$

The gas permeability is measured using core Lab permeameter followed methods adopted by [12]. Gas permeability measurements were conducted with Hassler type core holder in which samples (approximately 2.5 cm in diameter and 5 cm in length) were subjected to dry Nitrogen gas with pressure of 1378.9514 kpa the permeability is calculated by the following formula.

$$K = (C \cdot Q \cdot h_w \cdot L_2) / 200 V_b \quad (4)$$

Where: K is gas permeability, mD, L is the length of the sample, cm, h_w is the orifice manometer reading, mm, Q is the orifice value, c is the value of mercury height, mm, and V_b is the sample bulk volume, cm^3

γ -Ray Laboratory Measurements

The radiation from a rock sample is compared with the radiation from known standards. The accuracy and precision of the results depends on many factors [13] such as the size and energy resolution of the detector; the mass and geometry of the sample; the shielding of laboratory background; counting time; data processing procedures; and the quality of the radioactive standards. The slab core sample and detector are enclosed within 6-10 cm of lead shielding to reduce the background radiation. Modern computer techniques enable the full multichannel gamma ray processing of spectra. This eliminates spectrum drift by normalizing the data to reference gamma ray spectra. The relative concentrations of U and Ra in a sample can be used to estimate the radioactive equilibrium between these isotopes.

Formation Resistivity Factor

The electrical resistivity (R_o) was measured when samples were fully saturated by brine with water resistivity ($R_w = 0.071$ ohm.m) using of Core Lab Inc A.C. bridge (Model 100A). The measuring technique was outlined by [12]. Electrical resistance (r) of the samples was measured along the axis of cylindrical plug. Then, resistivity (R) was calculated from the measured resistance

(r) using the cross-sectional area of the core (A) and the length of the core (L). Formation factor was obtained as a ratio of rock resistivity (Ro) to brine resistivity (Rw) as:

$$F = Ro/Rw \tag{5}$$

Results and discussions

Porosity

The measured porosity values are ranged from 5.3% up 40.3% for the Saffron-2 field samples. The porosity frequency polygon is plotted (Fig. 3) showing bimodal distribution. It indicates two sample populations while the first has porosity mode value equals 12% and the second has porosity mode value equals 36.5%. The average porosity value is approximately of 24% which is high enough to store a huge gas volume. Porosity vertical profile (Fig. 4) shows in general, high porosity for the shallow sand channels and slightly low values for the deeper channels. This may be due to the increase of compaction with burial depth and its negative impact on porosity values. In the depth from 1870 up to 1915 there are no sand bodies and only silt and siltstone.

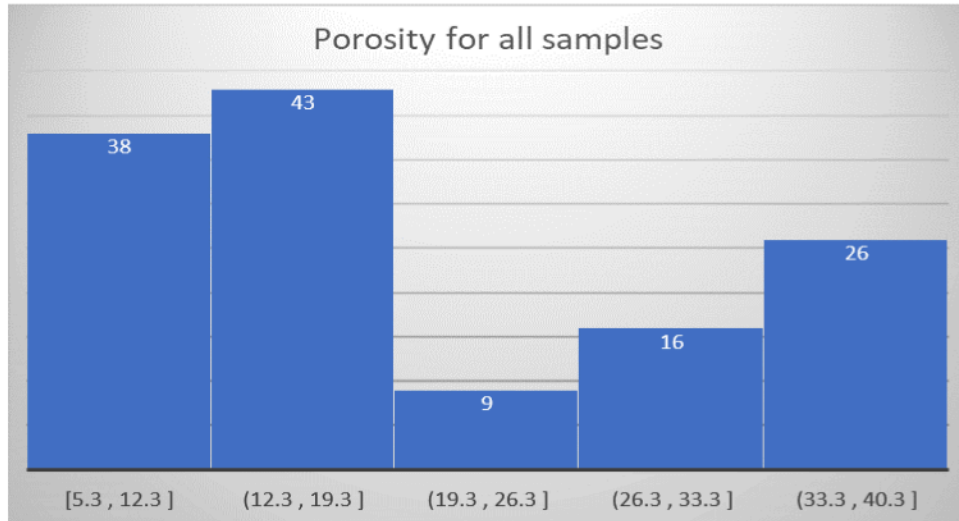


Fig. 3. Porosity frequency polygon

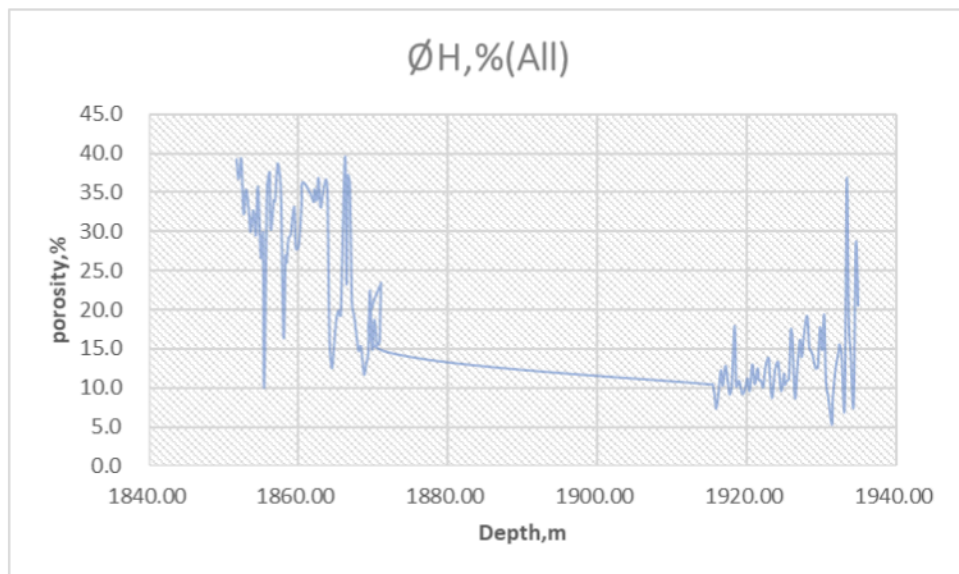


Fig. 4. Porosity vertical profile

Density

The measured rock grain density of Saffron -2 field was ranged from 2.2 g/cm³ up to 2.8 g/cm³ with average value equals 2.5 g/cm³. The measured data were drawn as frequency histogram (Fig. 5). It shows bimodal distribution confirming what have been obtained for porosity frequency distribution. It reveals that Saffron-2 sand channels are mainly composed of two sediment populations. The first has density mode value of 2.33 g/cm³, while the second has density mode value equals 2.59 g/cm³. These values designate that Saffron-2 sand bodies are not completely clean or clay/silt free. Fig. 6 exposes the vertical profile of grain density measured for samples of Saffron-2 field. Density curves reveal that there are more sand bodies of grain density = 2.65g/cm³ or more in the shallow depths, while in deeper conditions the quantity of sand bodies is reduced and replaced by siltstone and clay.

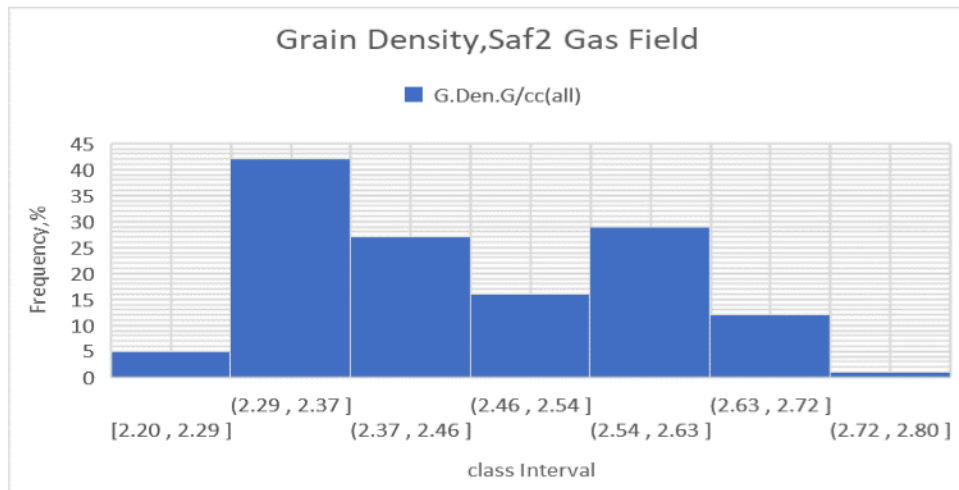


Fig. 5. Density frequency distribution

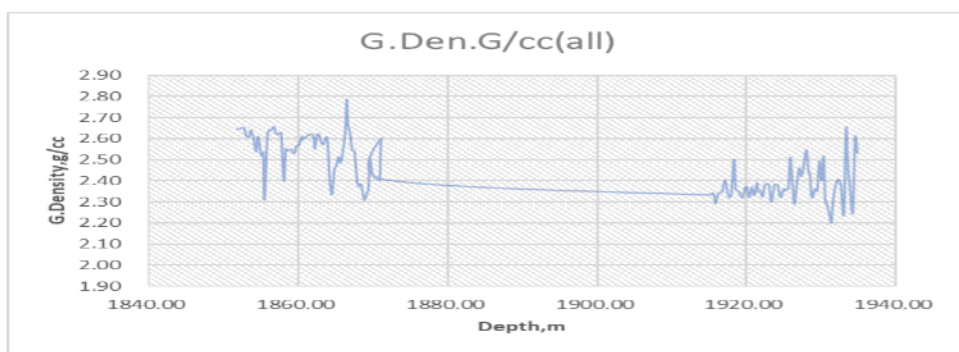


Fig. 6. Grain density vertical profile

Permeability

The measured permeability for 403 core samples of Saffron-2 field - core -2 was ranged from 0.0 up to 1950 mD. The frequency histogram represents the permeability distribution (Fig. 7) shows that most samples (339 samples) are filled in the first class ranged from 0.0 to 150.0 mD, while the rest are distributed along very wide range with few numbers. The permeability frequency distribution exposes a negative skewed distribution. Permeability of the Saffron-2 core-2 was plotted against depth to show its vertical profile (Fig. 8). It exhibits the permeability behavior of the saffron core-2 samples along depth.

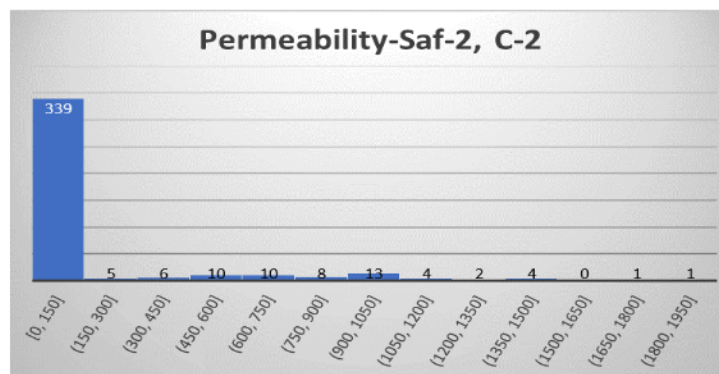


Fig. 7. Frequency distribution of permeability of C-2

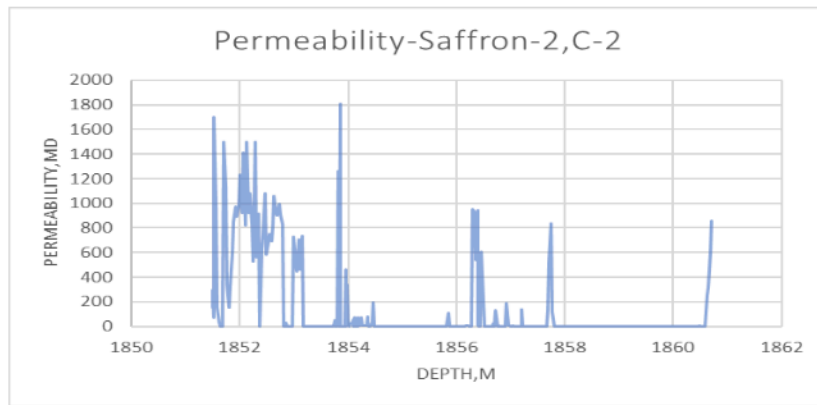


Fig. 8. Permeability of C-2 versus depth

Porosity versus Permeability

Porosity values were plotted versus permeability of Saffron-2 field (C2,3,4&C5) to show how much they are consistent and valuable in the well logging interpretation (Fig. 9). The calculated regression line equations were listed on the graph, while the orange color represents C3,4&5 and blue color exhibits only Saffron-2 C-2. Both regression line equations are reliable and robust ($R^2 = 0.79$) allowed to predict permeability from routine porosity values.

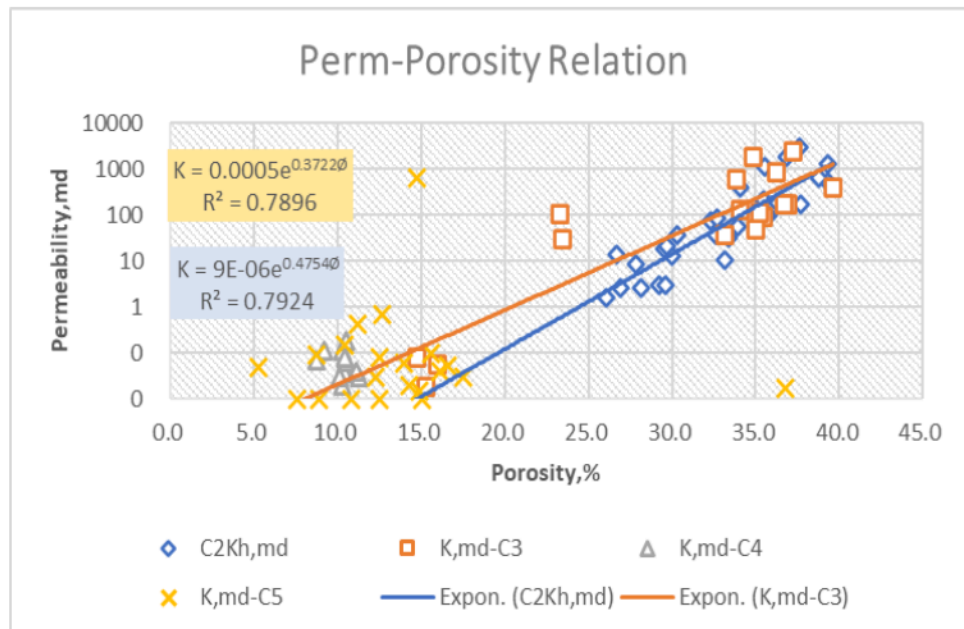


Fig. 9. Permeability versus Porosity for C2,3,4&5

Y- Ray Spectrum

The measured gamma values were ranged from 8.0 API^o up to 65API^o for all studied core samples (C2,3,4&5). With an average = 36.5 API^o. The frequency histogram exposes discrete polymodal distribution (Fig. 10). It indicates the presence of more than two rock populations, while one of them is highly predominant with the highest y-ray intensity ($\gamma > 45$ API^o).

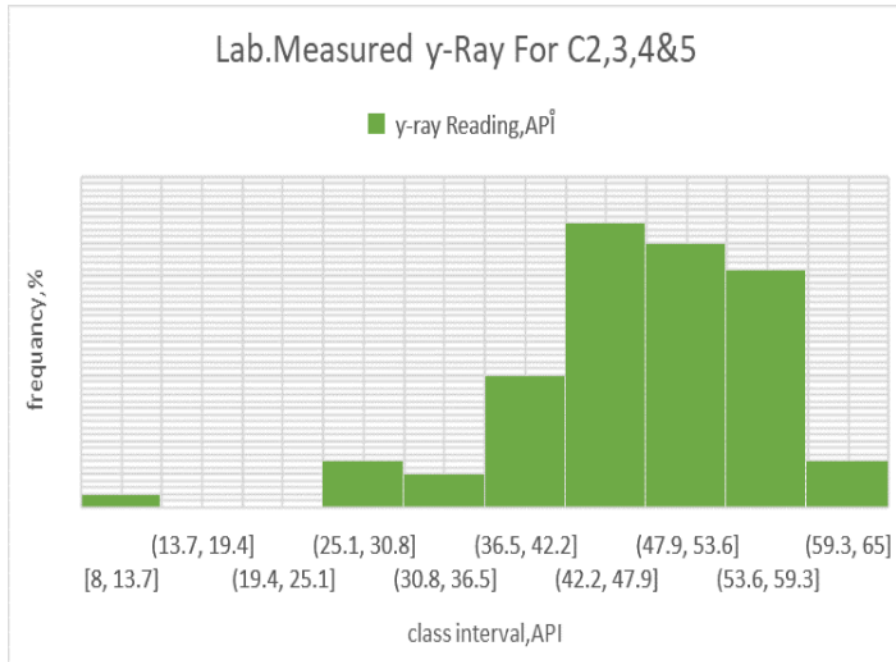


Fig. 10. γ -Ray frequency distribution

The vertical profile of the measured γ -Ray versus depth is shown (Fig. 11). It reveals that γ -Ray is higher in deeper parts (C-4 and C-5) than that in shallow depths. This is confirming the presence of siltstone and clay minerals rich with K^{40} and other isotopes.

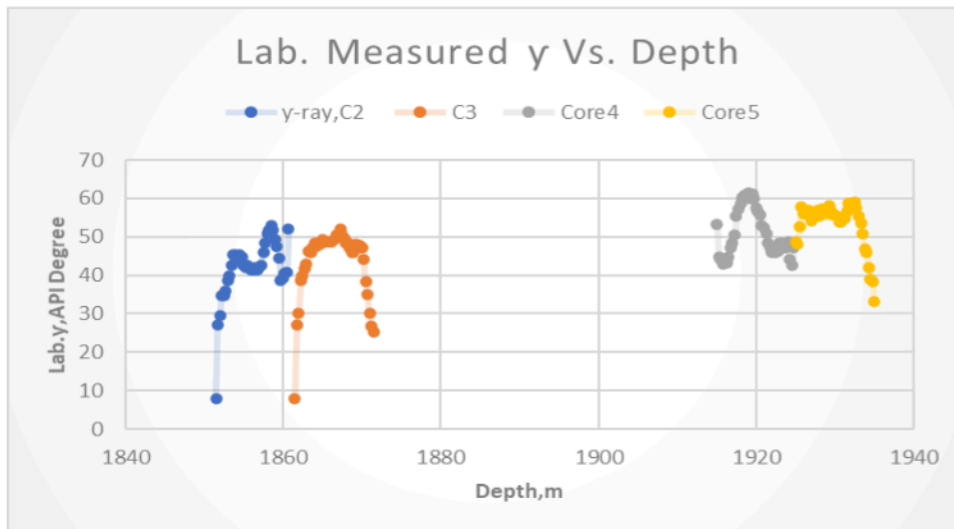


Fig. 11. Vertical profile of laboratory measured γ -Ray

Formation Resistivity Factor

The calculated formation resistivity factor of Saffron -2 field was ranged from 16.3 up to 49.3 and exhibits negative skewed distribution (Fig. 12). It is plotted against porosity and the calculated regression line equation is (Fig. 13):

$$F = 2.19 \varnothing - 0.9 \quad R^2 = 0.93 \quad (6)$$

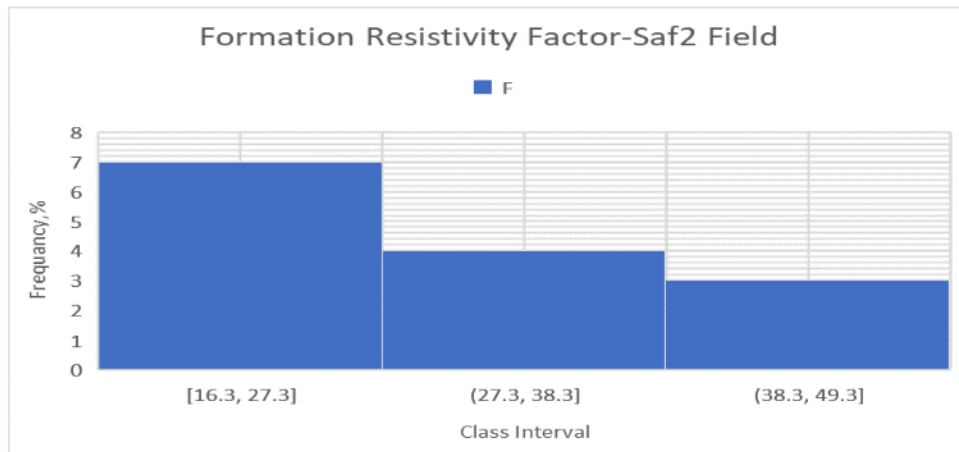


Fig. 12. Frequency distribution of formation factor

Porosity versus multiplier (a)

An attempt was made to relate porosity with the Archie's multiplier (a), while it shows positive relationship with fair coefficient of correlation ($R^2 = 0.5$). (Fig. 14)

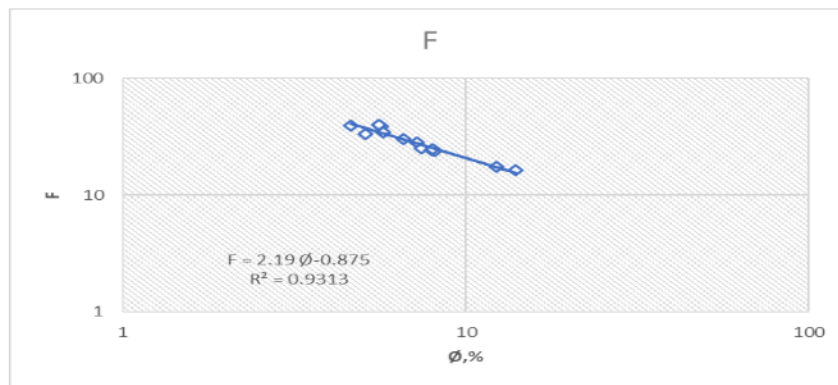


Fig. 13. Formation factor versus porosity

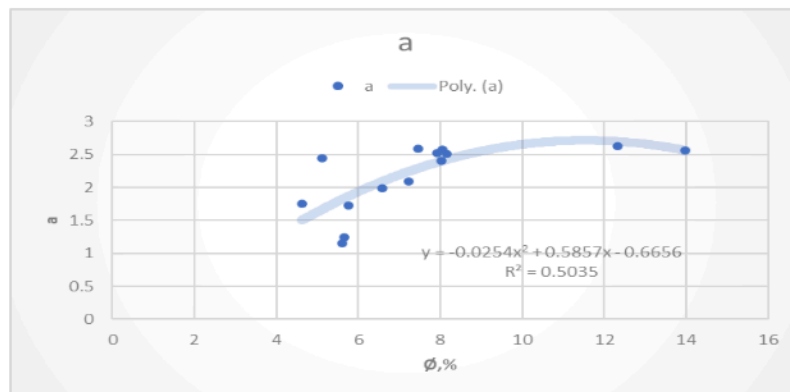


Fig. 14. Porosity versus Archie's multiplier (a)

Conclusions

- The increase of compaction with burial depth has a negative impact on both porosity and permeability values of the Saffron sand bodies.
- γ -Ray is higher in deeper parts (C-4 and C-5) than that obtained in shallow depths. This is confirming the presence of siltstone and clay minerals rich with K-40 and other isotopes.
- The calculated formation resistivity factor of Saffron -2 field was ranged from 16.3 up to 49.3 and exhibits negative skewed distribution.
- The multiplier (a) of the Archie's second law shows positive relationship with the Saffron sand porosity.

Acknowledgment

Authors wishing to acknowledge the PUR of Ain Shams University and EGPC for providing the data and permission for publication.

References

1. A. Samuel, Kneller, B., Raslan, S., Sharp, A., Parsons, C., 2003. Prolific deep-marine slope channels of the Nile Delta, Egypt. *Am. Assoc. Petrol. Geol. Bull.* 87, 541–560.
2. J.C. Harms, Wray, J.L., 1990. Nile Delta. In: Said, R. (Ed.), *The Geology of Egypt*. Balkema, Rotterdam, Netherlands, pp. 329–344
3. C. Vander, Cramer, B., Gerling, P., Winsemann, J., 2007. Natural gas formation in the western Nile delta (Eastern Mediterranean) : Thermogenic versus microbial. *Org. Geochem.* 38, 523–539.
4. A. Rizzini, Vezzani, F., Cococchetta, V., Milad, G., 1978. Stratigraphy and sedimentation of a Neogene–Quaternary section in the Nile Delta area (ARE). *Mar. Geol.* 27 (3–4), 327–348
5. M. Leila, Moscardello, A., 2017. Organic geochemistry of oil and natural gas in the west Dikirnis and El-Tamad fields, onshore Nile Delta, Egypt: Interpretation of potential source rocks. *J. Pet. Geol.* 40 (1), 37–58.
6. M. Sarhan, Hemdan, K., 1994. North Nile Delta structural setting and trapping mechanism, Egypt. In: *Proceedings of the 12th Egyptian General Petroleum co.*
7. A. Abdel Aal, El Barkooky, A., Gerrits, M., Meyer, H.J., Schwander, M., Zaki, H., 2001. Tectonic evolution of the Eastern Mediterranean basin and its significance for the hydrocarbon prospectivity of the Nile Delta deepwater area. *GeoArabia* 6 (3), 363–384.
8. EGPC (Egyptian General Petroleum Cooperation), 1994. Nile Delta and North Sinai. *Fields, Discoveries and Hydrocarbon Potentials (A Comprehensive Overview)*. Egyptian General Petroleum Corporation, Cairo, Egypt, 387 pp
9. W.S. El Diasty et al., 2020, Organic geochemistry of condensates and natural gases in the northwest Nile Delta offshore Egypt., *Journal of Petroleum Science and Engineering* 187 (2020) 106819
10. G. Sestina, 1995. Regional petroleum geology of the world part II: Africa, America, Australia 641, and Antarctica. *Gebrüder Bornträger Verlagsbuchhandlung, Stuttgart, Beiträge zur regionalen Geologie der Erde*, 22, 66–87.
11. EGPC, 1992. Western Desert oil and gas fields (A comprehensive overview). 11th EGPC 591 Petroleum Exploration and Production Conference, Egyptian General Petroleum 592 Corporation, Cairo, 431p.
12. A.M.A. El Sayed, A. A., Geological and petrophysical studies for Algyö -2 reservoir evaluation, Algyö oil and gas field, Hungary, Ph.D. Thesis, Hungarian Academy of Science, Budapest, 1981.
13. I.A.A., 1987. Preparation and Certification of IAEA Gamma ray Spectrometry Reference Materials RGU-1, RGTh-1 and RGK-1, Techn. Report-IAEA/RL/148, IAEA, Vienna.